ELSEVIER

Journal of Wind Engineering
and Industrial Aerodynamics 91 (2003) 1141–1154

JOURNAL OF wind engineering AND industrial aerodynamics

www.elsevier.com/locate/jweia

Concentration and flow distributions in urban street canyons: wind tunnel and computational data

Cheng-Hsin Chang[a,*], Robert N. Meroney[b]

[a] *Department of Civil Engineering, Tamkang University, 151 Ying-Chun Road, Tamsui, Taipei, Taiwan*
[b] *WEFL, Department of Civil Engineering, Colorado State University, Fort Collins, CO 80523, USA*

Received 20 August 2002; received in revised form 3 May 2003; accepted 10 June 2003

Abstract

The goal of this paper is to present bluff body flow and transport from steady point sources of pollutants, or chemical and biological agents in an idealized urban environment This paper includes ventilation behavior in different street canyon configurations. To evaluate dispersion in a model urban street canyon, a series of tests with various street canyon aspect ratios (B/H) are presented. Both open-country roughness and urban roughness cases are considered. The flow and dispersion of gases emitted by a point source located between two buildings inside an urban street canyon were determined by the prognostic model FLUENT using four different RANS turbulent closure approximations and in the model fire dynamics simulator using a large eddy simulation methodology. Calculations are compared against fluid modeling in the Industrial Meteorological Wind Tunnel at Colorado State University. A basic building shape, the Wind Engineering Research Field Laboratory building (WERFL) at Texas Tech University, was used for this study. The urban street canyon was represented by a 1:50 scale WERFL model surrounded by models of similar dimensions. These buildings were arranged in various symmetric configurations with different separation distances and different numbers of up- or downwind buildings. Measurements and calculations reveal the dispersion of gases within the urban environment are essentially unsteady, and they are not always well predicted by the use of steady-state prediction methodologies.

Keywords: Urban street canyon; Dispersion; Air pollution aerodynamics; Numerical modeling

*Corresponding author. Tel.: +886-2-2621-5656; fax: +886-2-2620-9747.
E-mail address: cc527330@ms56.url.com.tw (C.-H. Chang).

0167-6105/$ - see front matter © 2003 Elsevier Ltd. All rights reserved.
doi:10.1016/S0167-6105(03)00056-4

1. Introduction

The purpose of this paper is to present and critique the nature of bluff body flow and transport from steady point sources of pollutants, or chemical and biological agents in an idealized urban environment. The flow patterns that develop around individual buildings govern the wind forces on the building and the distribution pressure about the building and pollution about the building and in its wake. The superposition and interaction of flow patterns associated with adjacent buildings govern the final distribution of facade pressures and the movement of pollutants in urban and industrial complexes. Street canyon depth and width, intersection locations, canyon orientation to dominate wind directions and building geometries will determine peak pollution incidents [1].

Meroney et al. [2] provided a short review of the previous field and laboratory experience with flow and dispersion within and over urban structures. These studies identified many of the gross features of street canyon circulation, roof top separation regions, and elevated boundary layers which have become familiar to wind engineers. In addition, they focused on the need to use a stable and laterally homogenous line source to obtain consistent results while simulating vehicular pollution in an urban model study. Subsequently, Meroney et al. [3] reported the results of dispersion from such improved line sources in idealized two-dimensional urban configurations. Chang and Meroney [4–6] focused attention on the flow fields, building pressures and line source dispersion characteristics found for idealized three-dimensional urban arrays. Shelter effects within the canyons were found to be significant, such that flow patterns are displaced and mean and peak-induced loads are significantly different from the isolated building base case. Numerical simulations were compared to dispersion measurements from ground-level street-centered line sources. They revealed that the gross dispersion contours for different building configurations could be reproduced, but the steady-state CFD approach tended to overestimate street canyon wall concentrations.

Advanced technology makes computers faster and more powerful, which allows computational fluid dynamics (CFD) procedures to be applied to many experimental flow problems. Today, increasing applications of CFD to wind engineering problems include wind load of building and pollutant dispersion phenomena. Several previous studies have compared measurements made during physical modeling with numerical predictions. He and Song [7] simulated the wind flow around the Texas Tech University (TTU) building and roof corner vortex by using a large eddy simulation (LES) code. They claim that the three-dimensional roof corner vortex pattern was successfully simulated and that mean values of pressure predicted were in good agreement with wind tunnel and field test measurements. Murakami et al. [8] generated velocity fluctuations for an inflow boundary condition for LES with prescribed spatial correlation distributions and turbulence intensity levels. To generate velocity fluctuations for an inflow boundary condition for LES is one of the most important unresolved problems in CFD research. Lee et al. [9] solved for wind effects on a bluff body using the finite element method, and he compared simulated results with numerical and experimental studies reported by other researchers.

Selvam [10] used LES to compute the pressures around the TTU building using different inflow turbulence conditions, and he compared them with available field mean and peak pressure coefficients. Rehm et al. [11] compared mean surface pressure on a single building by using an LES algorithm with uniform and shear inflows. Cheatham et al. [12] also simulated the flow and dispersion around a surface-mounted cube, and they examined the effect of resolution, boundary conditions, and the form of the inflow velocity profiles. Carpenter and Locke [13] investigated wind speeds over multiple two-dimensional hills and compared results with numerical solutions.

Using RANS turbulence models, Meroney et al. [14,3] examined the behavior of line-source diffusion within two-dimensional arrays of simple rectangular model buildings. Leitl and Meroney [15] compared traffic exhaust dispersion in street canyons as measured by Rafailidis et al. [16] with numerical simulations including the effects of pitched roofs and finite length cross wise streets. Leitl et al. [17] considered the numerical simulation of concentration and flow distributions in the vicinity of U-shaped building structures. They compared their calculations against detailed wind tunnel measurements produced by Klein et al. [18]. Delaunay et al. [19] compared the numerical and wind tunnel simulation data of point sources located at different position on the top of a rectangular building.

1.1. Wind tunnel modeling

This study used a basic building shape, the Wind Engineering Research Field Laboratory building (WERFL) at TTU, Lubbock to build an urban street canyon model. Pressure fields, flow and dispersion patterns about this isolated building have been extensively measured both at full scale and over various model scales immersed in an equivalent turbulent shear layer [20–23].

A plastic model of the WERFL structure was constructed to a 1:50 scale and instrumented with multiple pressure ports. A large number of "dummy" models of similar dimensions were constructed of plastic foam and wood to represent surrounding buildings. These buildings were arranged in various symmetric configurations with different separation distances, and then they were placed in the Industrial Wind Tunnel (IWT) of the Wind Engineering and Fluid Laboratory, Colorado State University. Typical building patterns are noted in Fig. 1, and the associated arrangement patterns are listed in Table 1. Upwind of the building array entrance region spires and surface roughness conditioned the approach boundary layer to simulate a rural approach wind profile power law of $n = 0.14$ and a building height turbulent intensity of 22% [24].

Flow visualization was accomplished with a laser-light sheet produced by 5 W Coherent Innova 7005 Argon ion water-cooled laser. Images were recorded by using a Panasonic Omni vision II camera/recorder system. A point source was located at the center point of a cross street canyon in front of the base building model. The dimensionless concentration coefficient used in the presentation of the data is $K = CUH^2/Q$, where C is the dimensional tracer species volume fraction, U is the upwind free stream velocity at roof height, H is the building height and Q is the

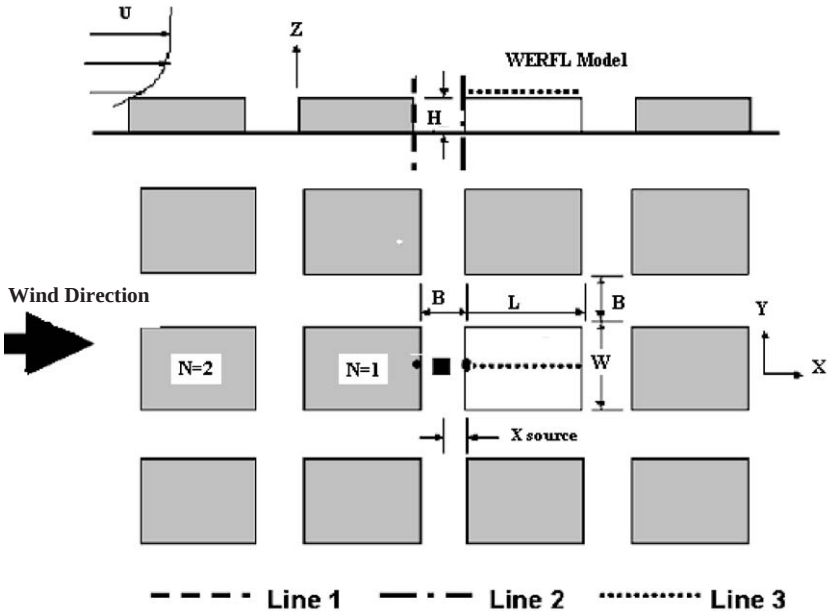

Fig. 1. Schematic of urban street-canyon model arrangement concentrations of tracer gases (C_2H_6) released from point source regions were measured using an Hewlett Packard 5710A flame-ionization gas chromatography. An automated sampling system using 50 syringes captured samples simultaneously for sequential processing through the gas chromatography. Transducer voltages were integrated and recorded automatically by a LabVIEW based data acquisition system.

Table 1
Array of model structures studied, $X_{source} = B/2$

B/H	λ_{area} [a]	$\lambda_{frontalarea}$ [b]	N rows	Structure	Flow
0.5	0.72	0.21	1, 2, 3, and 8	City center	Skimming flow
1.0	0.54	0.16	1, 2, 3, and 8	City center	Skimming flow
2.0	0.34	0.10	1, 2, 3, and 8	Suburban	Wake interface
4.0	0.17	0.05	1, 2, 3, and 8	Urban 1-2 stories	Wake interface
6.0	0.10	0.03	1, 2, 3, and 8	One-story houses	Isolated

[a] $\lambda_{area} = \Sigma$Areas covered by buildings/total urban area.
[b] $\lambda_{frontal\ area} = \Sigma$Building area normal to wind/total urban area.

source flow rate. It is known that the horizontal wind velocity at street level is typically of the order of 10% the free stream velocity. For reference velocities achievable in the IWT, this results in horizontal velocities at street level of a few cm/s. Simple calculations show that the tracer gas discharge velocities from the point source are the same order of magnitude, so they may influence the recirculating flow

patterns in the canyon. To reduce this source interaction a lid or cap was placed directly above the source inlet to reduce vertical velocities.

1.2. Numerical modeling

The computational programs FLUENT and fire dynamics simulator (FDS) were used for numerical simulations. The intent of the numerical simulations were to validate the CFD models, compare the different CFD approaches, and determine intrinsic limitations to steady or unsteady prediction procedures. The FLUENT CFD software is based on a finite volume discretization of the equations of motion, an unstructured grid volume made either of rectangular prisms or tetrahedral cells, various matrix inverting routines, and in this case either k-epsilon ($k-\varepsilon$), renormalized group theory k-epsilon ($k-\varepsilon$), Reynolds stress, or Spalart-Almaras turbulence models [25]. A complete description of the model, many validation examples, and a bibliography of published papers and reports may be found on the web at http://www.fluent.com.

The FDS CFD software developed by McGrattan et al. [26] solves an approximate form of the Navier–Stokes equations appropriate for low Mach number applications. A description of the model, many validation examples, and a bibliography of related papers and reports may be found on the web at http://www.nist.gov/fds. The LES turbulence model used by FDS permits one to specify either no slip or half-slip boundary conditions for near-boundary velocities. The half-slip assumption has often been found appropriate in situations where refined grids are not convenient due to total grid matrix size limitations imposed by computational resources.

For the current application for both CFD programs, the point source inlet was modeled as a 1.3×1.3 cm vent emitting at a constant velocity and no turbulence. The inlet velocity of $w_{\text{source}} = 0.05$ m/s was set to be equivalent to the source emission rate used in the wind tunnel simulation. A tracer mass fraction of 1 was applied to the point source inlet during the calculation. In presenting the results from the calculation, tracer species density was normalized to facilitate comparison with experiments and other numerical results.

2. Results and discussion

Depending on the street width to building height ratio (B/H), the flow in the street canyons can be classified as skimming flow ($B/H = 0-1.2$), wake interference flow ($B/H = 1.2-5.0$), or an isolated roughness flow ($B/H > 5.0$) as originally proposed by Oke [27]. Through the observation of flow visualization of wind tunnel tests, the results match the observations made by Oke. Fig. 2 exhibits the skimming flow image of case $B/H = 1$. Fig. 3 is an example of interference flow case ($B/H = 4$ case) and Fig. 4 is an example of isolated roughness flow (case $B/H = 6$). Extended comparisons of the magnitudes measured for wind and turbulence profiles may be found in [24]. Building pressure distributions can also be examined in [6].

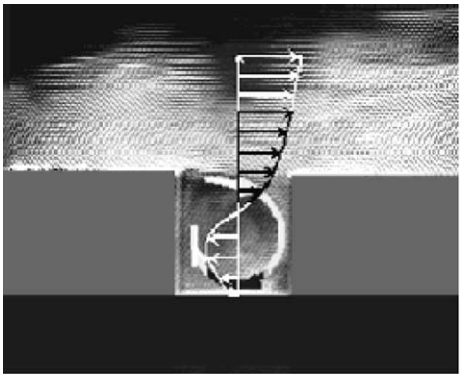

Fig. 2. Skimming flow, $B/H = 1$.

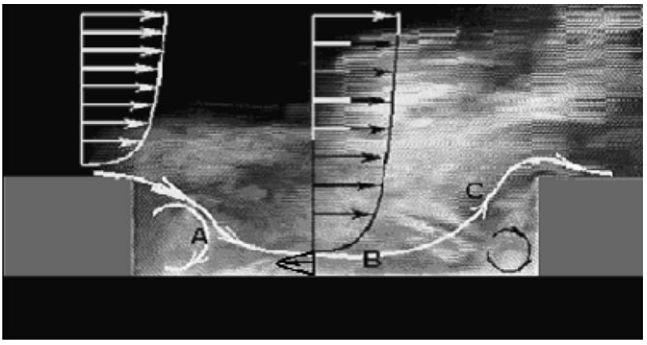

Fig. 3. Interference flow, $B/H = 4$.

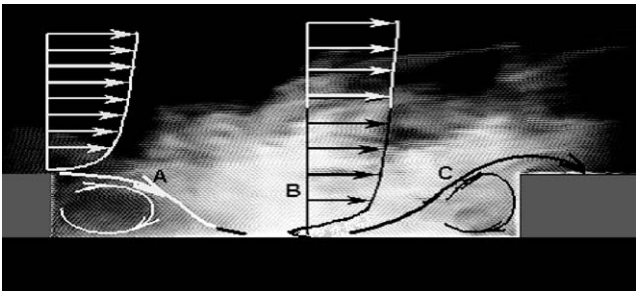

Fig. 4. Isolated roughness flow, $B/H = 6$.

Fig. 5 shows the normalized concentrations on the centerline of the upwind and downwind walls of street canyons for $B/H = 0.5$ and different numbers of building rows, N. The normalized concentrations generally larger for the $B/H = 0.5$ case, especially in the street-level corners of the canyons. However, the largest

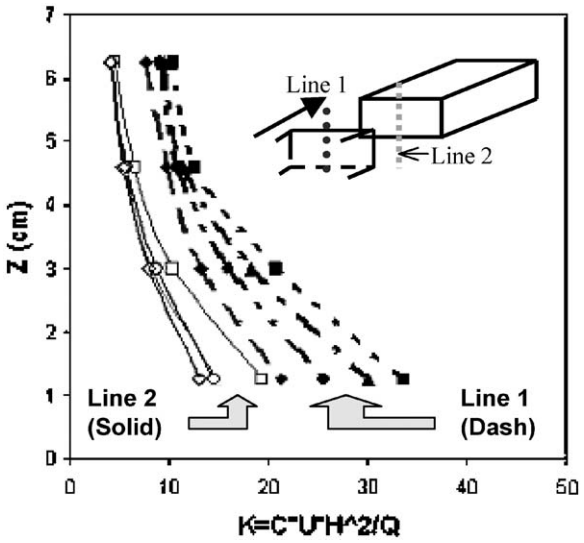

Fig. 5. Concentrations on the upwind and downwind walls for case $B/H = 0.5$.

concentrations were actually measured for $B/H = 1.0$ and $N = 8$ on measurement Line 1. The upwind wall areas have higher concentrations than the downwind wall areas, because there are two circulation flows inside the street canyon: the upper circulation flow is clockwise and the lower circulation flow is counter-clockwise. The circulation carries the emission gas to the upwind wall of the street canyon, resulting in higher concentrations on the upwind wall. The lower circulation flow (CCW) carries some emission to the downwind wall of the street canyon, so the ground corner of the downwind wall also has high concentrations. The results also show that the open-country roughness cases ($N = 1, 2$) have higher concentrations at street level than the urban roughness cases ($N = 3, 8$).

Similarly, Fig. 6 shows normalized concentrations for $B/H = 1$ with different number of rows, N. Since there is only one circulation eddy (CW) in the street canyon, the clockwise flow impinges on the upwind wall areas. Therefore, the upwind wall areas have higher concentrations than the downwind wall areas. Contrary to the cases of $B/H = 0.5$, the higher concentrations occur for the street canyons of the urban roughness cases ($N = 3, 8$) instead of the open-country roughness cases ($N = 1, 2$). It is likely that with fewer upwind buildings and a broader street canyon (i.e. $N \leqslant 2$), the flow field is more unstable and intermittent ventilation of the entire canyon occurs more often resulting in lower street-level concentrations. It is possible the added upwind buildings provide additional sheltering and produce flows which less frequently dip into the street cavities which permit higher average concentrations against the upwind wall.

Figs. 7 and 8 both show interference flow effects on the concentrations for the cases $B/H = 2$ and 4, respectively. Similar to the cases of $B/H = 0.5$ and 1, both $B/H = 2$ and 4 show that the upwind wall areas have higher concentrations. Wake

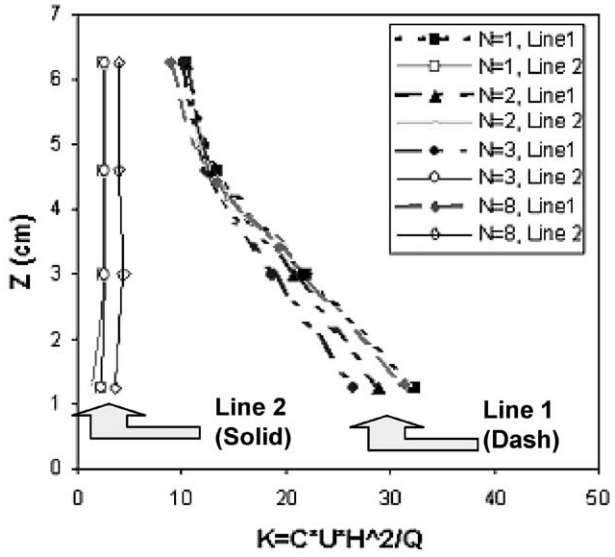

Fig. 6. Concentrations on the upwind and downwind walls for case $B/H = 1$.

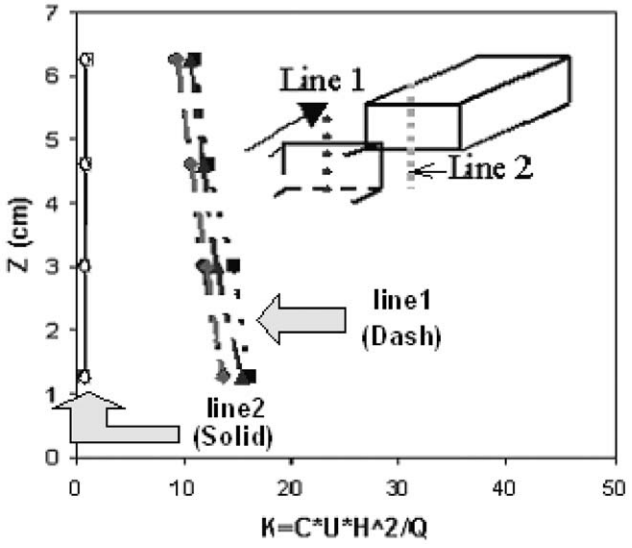

Fig. 7. Concentrations on the upwind and downwind walls for case $B/H = 2$.

zone eddies occurring against the upwind wall areas and the resulting recirculation impinges the gas against upwind wall areas. However, with greater width of the street canyons, the downwind wall areas have very low concentrations, because the circulation downwind of the upwind eddy carries the emissions out of the canyons.

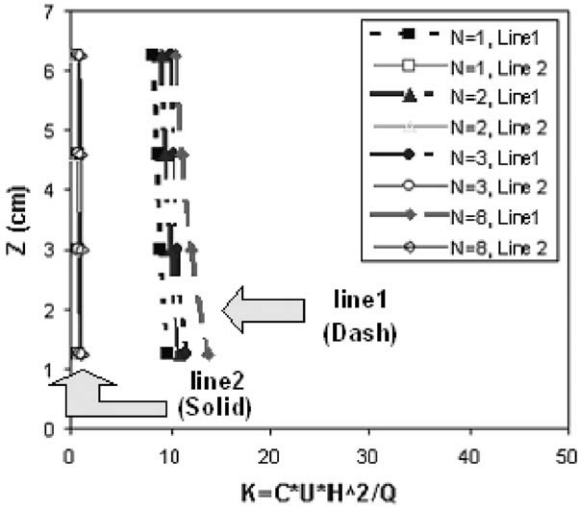

Fig. 8. Concentrations on the upwind and downwind walls for case $B/H = 4$.

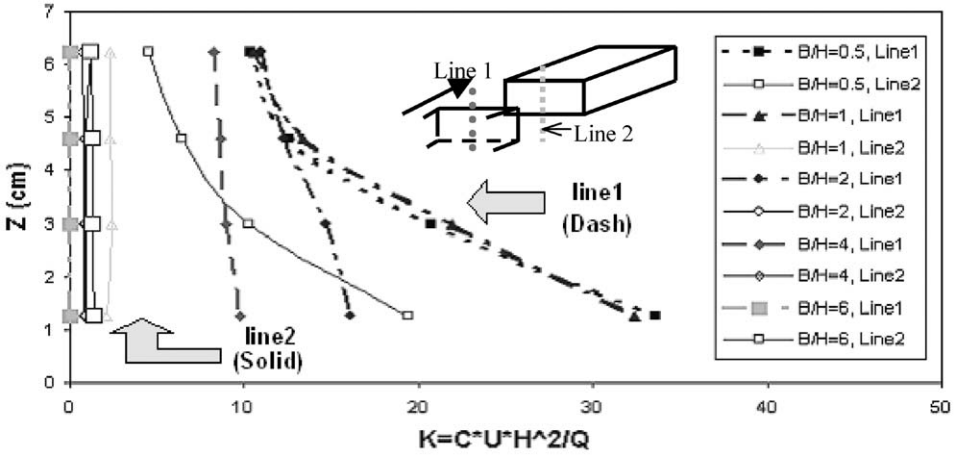

Fig. 9. Concentrations on the upwind and downwind walls of the street canyon for open-country roughness case $N = 1$.

The concentrations are higher for $B/H = 2$ than for $B/H = 4$ because the dilution effects in the cavity zone are higher for $B/H = 4$.

For the isolated roughness cases ($B/H = 6$), the concentrations are almost zero on the upwind wall areas of the street canyon, because the emissions are transported out of the canyon. The downwind wall areas, on the other hand, have higher concentrations because the concentrations convect to downwind wall areas directly. Fig. 9 presents comparisons of concentration levels for $N = 1$, but different B/H.

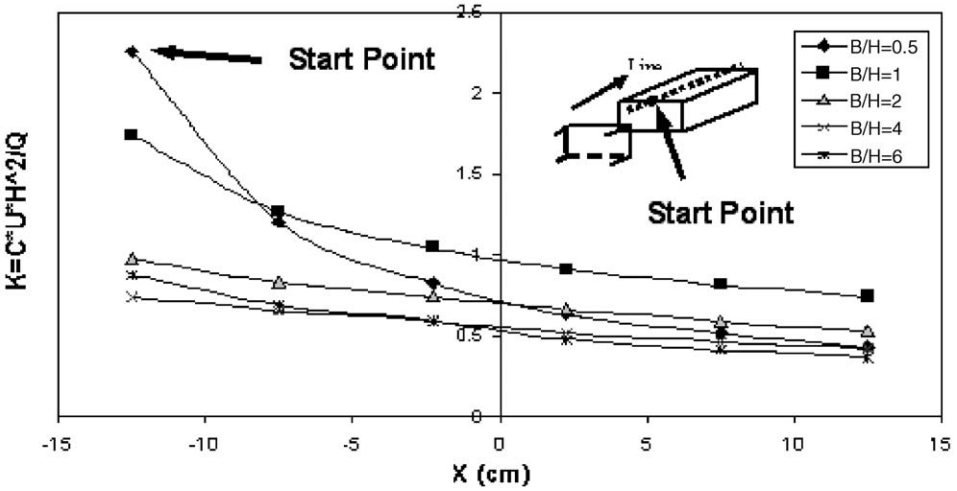

Fig. 10. Concentrations on the centerline of the roof for open-country roughness case $N = 1$.

The results show that the lower the ratio of B/H, the higher the concentrations in the street canyons.

Fig. 10 presents the concentration levels on the centerline of the roof area for $N = 1$ and different B/H values. The results of each case show that the concentrations become lower on the centerline of the roof as the distance along the roof become larger.

3. Comparison of wind tunnel results and numerical results

In this section, the numerical results were calculated by using different combinations of turbulence models, boundary conditions and grid resolution to optimize the best fit to the comparison results.

A comparison of each set of data from wind tunnel experiments with the numerical simulation reveals that the CFD software, FLUENT 5.4, can predict many of the wind tunnel results for average flow field, average pressure coefficients and in some cases average concentrations by choosing appropriate boundary condition, grid resolution and turbulence model. As part of an examination of the sensitivity of the numerical results to various computational alternatives, calculations were performed at different grid resolutions, wall boundary conditions, and different turbulence models to assure there were no trends or variations association with such numerical alternatives. Fig. 11 shows a direct comparison between measured and calculated concentrations on the centerline of the upwind and downwind walls for a street canyon for a point source inlet located mid canyon for all cases and $N = 1$. FLUENT gives higher concentration

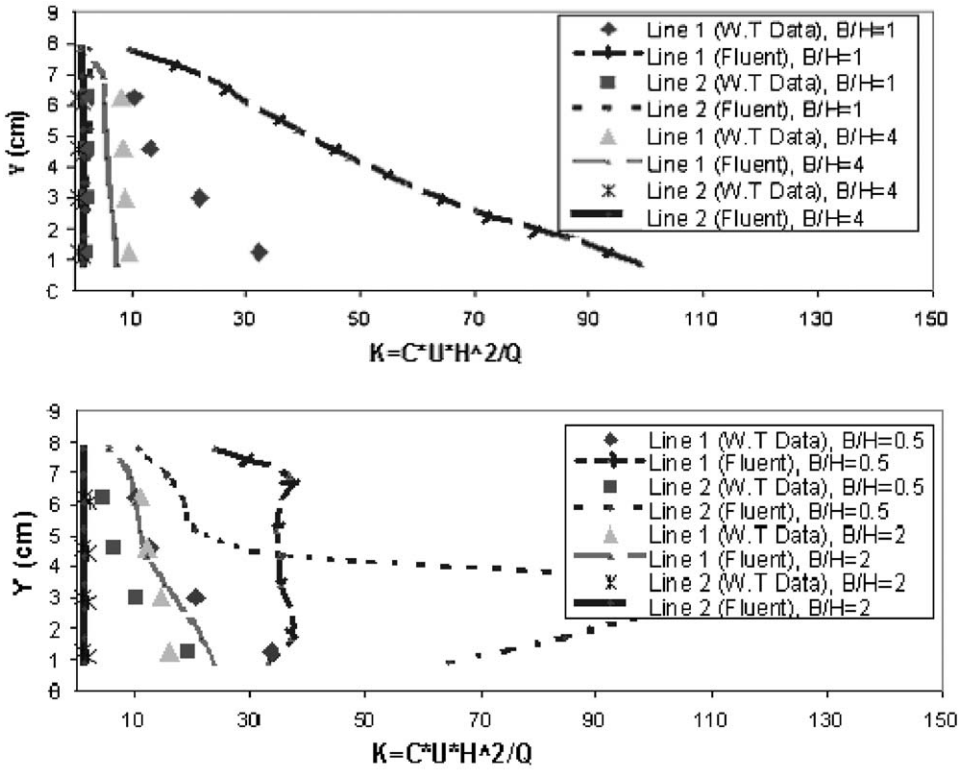

Fig. 11. Comparisons between wind tunnel and numerical model (FLUENT $\kappa - \varepsilon$ model) concentrations for the open-country roughness case $N = 1$.

predictions in some zones, for example, the ground-level corners of the upwind walls of $B/H = 1$ cases and the ground corners of both upwind and downwind walls of the $B/H = 0.5$ cases.

For FDS simulations, two ground boundary conditions are chosen to compare results with the wind tunnel measurements. Fig. 12 presents comparisons between wind tunnel and numerical concentrations for the centerline of the upwind and downwind walls of the open-country roughness case, $N = 1$ and $B/H = 1$. The result shows that with the half-slip ground boundary condition, the FDS more frequently predicts the measurements of the wind tunnel experiments. The calculated normalized concentrations from both FLUENT and FDS are plotted against the experimental normalized concentrations in Fig. 13. There is a near-linear relationship between the experimental and the numerical data. The slope of the line of best fit is 2.85 for FLUENT and 1.15 for FDS. The results from the FDS simulation agree much better with the experimental results than those from FLUENT.

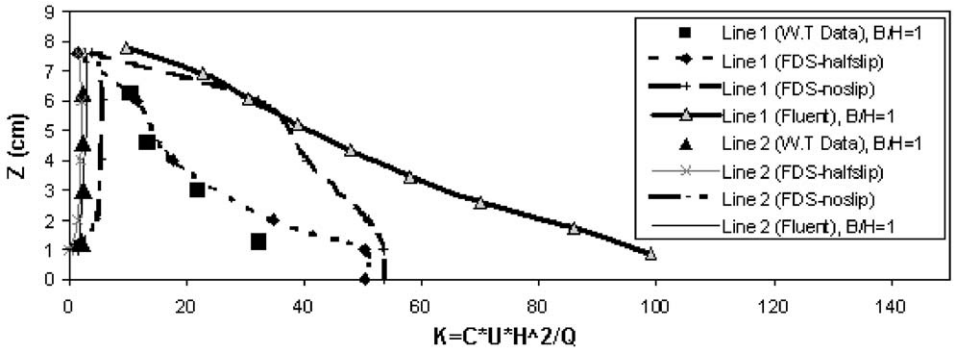

Fig. 12. Comparisons between wind tunnel and numerical model (FLUENT $\kappa-\varepsilon$ model, FDS) concentrations for the open-country roughness case $N=1$ and $B/H=1$.

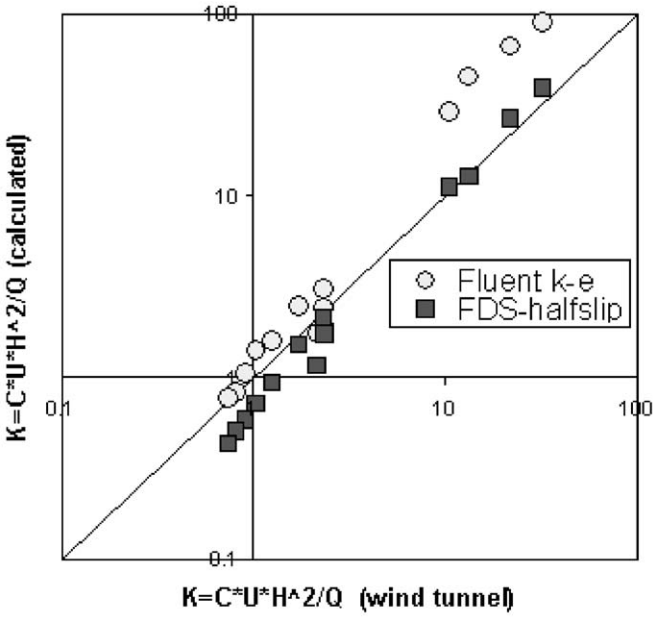

Fig. 13. Experimental vs. calculated (FLUENT and FDS) normalized concentration, K, on the centerline of the roof and upwind and downwind walls of canyon taps ($B/H=1$, $N=1$).

4. Conclusion

Significant pollution concentrations are usually measured on upwind walls of urban street canyons and along the downwind rooftops, but when multiple rolls occur in narrow canyons ($B/H=0.5$) it is possible for the plumes to be directed

toward the downwind canyon wall. As the street widths widen with respect to building height, wake-interference flows dominate the advection and dispersion of pollutant plumes. Once the street width to building height exceeds about 5, the flow field even for a multiple building arrangement, appears to be perturbed by individual isolated buildings. The higher pollutant concentration measured on upwind wall for wake-interference flows is that the pressure is low and tends to suck pollutant into cavity zone, close to upwind wall. For isolated building case, the higher concentrations happen at downwind wall, since there is no wake zone to carry pollutant to upwind.

The CFD programs reproduced the overall flow fields observed during the measurement program, but it is evident that steady-state calculations are not reproducing the intermittent nature of the penetration of elevated flows down into the canyons. This results in situations where the FLUENT CFD concentrations overpredict magnitudes along canyon walls. The FDS CFD program is inherently a time-dependent calculation; however, it is found that wall magnitudes can be very sensitive to the rather crude wall boundary conditions incorporated in the program.

Acknowledgements

The contribution of Dr. David E. Neff in implementing the experimental facilities at CSU is gratefully acknowledged. This work was supported by the US National Science Foundation through the CSU/TTU Cooperative Program in Wind Engineering, Grant No. CMS-9411147.

References

[1] W. Theurer, Point sources in urban areas: modeling of neutral gas clouds with semi-empirical models, in: Cermak, et al., (Eds.), Wind Climate in Cities, Kluwer Academic Publishers, Dordrecht, 1995, pp. 485–502.

[2] R.N. Meroney, M. Pavageau, S. Rafailidis, M. Schatzmann, Study of the line source characteristics for 2-D physical modeling of pollutant dispersion in street canyons, J. Wind Eng. Ind. Aerodyn. 62 (1996) 37–56.

[3] R.N. Meroney, S. Rafailidis, M. Pavageau, Dispersion in idealized urban street canyons, in: Gryning, Schiermeir (Eds.), Air Pollution Modeling and Its Application, Vol. XI, Plenum Press, New York, 1996, pp. 451–458.

[4] C.H. Chang, R.N. Meroney, Numerical and physical modelling of urban street canyon dispersion, in: S.-E. Gryning, F.A. Schiermeier (Eds.), Millennium NATO/CCMS International Technical Meeting on Air Pollution Modelling and its Application, Boulder, CO, May 15–19, 2000, Air Pollution Modeling and its Application, Vol. XIV, Kluwer Academic Publishers, New York, 2001, pp. 733–734.

[5] C.H. Chang, R.N. Meroney, Numerical and physical modeling of bluff body flow and dispersion in urban street canyons, J. Wind Eng. Ind. Aerodyn. 89 (2001) 1325–1334.

[6] C.H. Chang, R.N. Meroney, The effect of surroundings with different separation distances on surface pressures on low-rise buildings, First American Conference on Wind Engineering, Clemson University, South Carolina, June 4–6, 2001, 10pp.

[7] J. He, C.C.S. Song, A numerical study of wind flow around the TTU building and the roof corner vortex, J. Wind Eng. Ind. Aerodyn. 67–68 (1997) 547–558.

[8] T. Maruyama, Y. Maruyama, Large eddy simulations around a rectangular prism using artificially generated turbulent flows, Abstracts of Papers at Third International Symposium on Computational Wind Engineering, University of Birmingham, UK, September 4–7, 2000, pp. 11–14.
[9] S. Lee, Unsteady aerodynamic force prediction on a square cylinder using k–ε turbulence models, J. Wind Eng. Ind. Aerodyn. 67–68 (1997) 79–90.
[10] R.P. Selvam, Computation of pressures on Texas Tech University building using large eddy simulation, J. Wind Eng. Ind. Aerodyn. 67–68 (1997) 647–657.
[11] R.G. Rehm, K.B. McGrattan, H.R. Baum, E. Simiu, An efficient large eddy simulation algorithm for computational wind engineering: application to surface pressure computations on a single building, NISTIR 6371, Building and Fire Research Laboratory, NIST, Gaithersburg, MD, Website: http://fire.nist.gov.
[12] S.A. Cheatham, B.Z. Cybyk, J.P. Boris, Simulation of flow and dispersion around a surface-mounted cube, Naval Research Laboratory, Washington, DC.
[13] P. Carpenter, N. Locke, Investigation of wind speeds over multiple two-dimensional hills, J. Wind Eng. Ind. Aerodyn. 83 (1999) 109–120.
[14] R.N. Meroney, D.E. Neff, B. Birdsall, Wind-tunnel simulation of infiltration across permeable building envelopes: energy and air pollution exchange rates, Seventh International Symposium on Measurement and Modeling of Environmental Flows, International Mechanical Engineering Conference, San Francisco, November 12–17, 1995, p. 8.
[15] B. Leitl, R.N. Meroney, Car exhaust dispersion in a street canyon: numerical critique of a wind-tunnel experiment, J. Wind Eng. Ind. Aerodyn. 67–68 (1997) 293–304.
[16] R. Rafailidis, M. Schatzmann, Physical modeling of car exhaust dispersion in urban street canyons, Proceedings of the 21st International Meeting on Air Pollution Modeling and Its Applications, Baltimore, November 6–10, 1995.
[17] B. Leitl, P. Kastner-Klein, M. Rau, R.N. Meroney, Concentration and flow distributions in the vicinity of U-shaped buildings: wind-tunnel and computational data, J. Wind Eng. Ind. Aerodyn. 67–68 (1997) 745–755.
[18] P. Kastner-Klein, R. Rockle, E.J. Plate, Concentration estimation around point sources located in the vicinity of U-shaped buildings and in a built-up area, Second International Conference Air Pollution, Barcelona, Spain, September 27–29, 1994.
[19] D. Delaunay, Numerical and wind tunnel simulation of gas dispersion around a rectangular building, J. Wind Eng. Ind. Aerodyn. 67–68 (1997) 721–732.
[20] L.S. Cochrane, Wind-tunnel modeling of low-rise structures, Ph.D. Thesis, Department of Civil Engineering, Colorado State University, 1992, p. 348.
[21] J.B. Birdsall, Physical simulation of wind-forced natural ventilation, Master Thesis, Department of Civil Engineering, Colorado State University, 1993.
[22] H.J. Ham, Turbulence effects on wind-induced building pressures, Ph.D. Dissertation, Department of Civil Engineering, Colorado State University, 1998, p. 275.
[23] Banks, D. The suction induced by conical vortices on low-rise buildings with flat roofs, Ph.D. Thesis, Department of Civil Engineering, Colorado State University, 2000.
[24] H.C. Chang, Numerical and physical modeling of bluff body flow and dispersion in urban street, Ph.D. Thesis, Department of Civil Engineering, Colorado State University, 2001, p. 242.
[25] Fluent 5: User's guide, July 1998, Fluent Incorporated, Website: http://www.fluent.com.
[26] K.B. McGrattan, H.R. Baum, R.G. Rehm, A. Hamins, G.P. Forney, Fire dynamics simulator, Technical Reference Guide, Technical Report NISTIR 6467, National Institute of Standards and Technology, Gaithersburg, Maryland, 2000, 37pp, NIST Website: http://www.nist.gov/fds/.
[27] T.R. Oke, Street design and urban canopy layer climate, Energy Buildings 11 (1998) 103–113.